The New DØ Level-1 Calorimeter Trigger

M. Abolins[1], M. Adams[2], T. Adams[3], E. Agulio[4], L. Bagby[5], J. Ban[6], E. Barberis[7], S. Beale[8], J. Benitez[1],
J. Biel[1], R. Brock[1], J. Bystricky[9], D. Calvet[9], S. Cihangir[5], M. Cwiok[10], D. Edmunds[1], H. Evans[11], C. Fantasia[7],
J. Foglesong[5], J. Green[5], J. Hegeman[12], R. Kehoe[13], P. Laurens[1], P. Le Dû[9], C. Johnson[6], S. Lammers[6],
J. Mitrevski[6], M. Mulhearn[6], M. Naimuddin[14], B. P. Padley[15], J. Parsons[6], G. Pawloski[15], E. Perez[9], P. Renkel[13],
A. Roe[7], W. Sippach[6], A. Stone[5], G. Tarte[9], W. Taylor[8], R. Unalan[1], N. Varelas[2], H. Weerts[1], D. Wood[7],
L. Zhang[6], T. Zmuda[5]

Abstract— With increasing Tevatron luminosity, efficient triggers that meet the bandwidth limitations of the experiment's data acquisition system become more and more difficult to construct. To meet these challenges, the DØ experiment has significantly enhanced its triggering capabilities. A major component of this upgrade is a completely re-designed Level-1 Calorimeter Trigger (L1Cal). This new system uses novel architecture and algorithms to maintain acceptable background rejection while preserving or even improving signal efficiency at the highest luminosities foreseen. We describe interesting features of the L1Cal and give highlights from its first few months of operation.

Index Terms— IEEEtran, Dzero, Trigger, Calorimeter, Sliding Windows.

I. INTRODUCTION

THE Fermilab Tevatron recently completed a series of upgrades and, in June 2006, began its phase of high-luminosity operation known as Run IIB. At the DØ experiment, we installed an entirely new Level-1 Calorimeter Trigger for Run IIB, replacing the system which was originally built for Run I and continued to be used in Run IIA. The need for the new trigger was evident because extrapolations to Run IIB luminosities indicated that the rate from the old trigger would exceed the throughput capabilities of the data acquisition (DAQ) system, even for a physics program focused on high-p_t processes. The new trigger achieves greater background rejection through the use of sliding windows algorithms to identify jet, electromagnetic (EM), and tau physics objects and measure their transverse energies (E_t). The new trigger also extends the physics menu to include topological triggers (for example, acoplanar jets) and provides the calorimeter input to a new trigger system which matches calorimeter objects with tracks at Level 1. In addition, because experiments at the LHC also plan to use sliding windows algorithms, our experience with this trigger at DØ has broader impact beyond the Tevatron.

[1] Michigan State University, East Lansing, MI, USA [2] University of Illinois at Chicago, Chicago, IL, USA [3] Florida State University, Tallahassee, FL, USA [4] University of Alberta, Edmonton, Alberta, Canada [5] Fermi National Accelerator Laboratory, Batavia, IL, USA [6] Columbia University, New York, NY, USA [7] Northeastern University, Boston, MA, USA [8] York University, Toronto, Ontario, Canada [9] Service de Physique des Particules, DAPNIA/CEA, Saclay, France [10] University College Dublin, Dublin, Ireland [11] Indiana University, Bloomington, IN, USA [12] NIKHEF, Amsterdam, The Netherlands [13] Southern Methodist University, Dallas, TX, USA [14] Delhi University, Delhi, India [15] Rice University, Houston, TX, USA

An overview of the DØ Level-1 Calorimeter Trigger upgrade is shown in Figure 1. The Baseline Subtractor (BLS) system performs baseline subtraction for the precision readout, and constructs analog sums of calorimeter cell energies to produce analog trigger-pickoff signals with an η-ϕ resolution of 0.2×0.2. A passive transition system adapts the low-density BLS signals to the high-density inputs received on the ADC plus Digital Filter (ADF) cards. The ADF cards digitize and pedestal subtract the trigger-pickoff signals, forwarding the results to the Trigger Algorithm Boards (TABs). The TABs perform the sliding windows algorithms, providing regional sums of identified jet, EM, and tau physics objects to a single Global Algorithm Board (GAB). The GAB produces trigger terms (called and/or terms) for the global DØ Level-1 Trigger.

II. SLIDING WINDOWS ALGORITHMS

The sliding windows algorithm finds jet or electromagnetic (EM) objects by determining the calorimeter regions that contain local maxima of transverse energy deposits. Our implementation (see Figure 2) begins with a cluster sum algorithm which sums the digitized trigger-tower energies in a window surrounding each trigger-tower location. The window geometry is optimized for the type of physics object. In the next stage, the cluster sums associated with each trigger-tower location are compared with neighboring sums to find local maxima. Requiring a minimal space between local maxima, or de-clustering, is accomplished by extending the local maxima comparison beyond the nearest neighbors. Finally, the object E_t is determined by adding additional trigger-tower energies to the cluster sum, again based on geometry optimized to the physics object.

A. Jets

Jet objects are broad and deposit energy in both the electromagnetic and hadronic portions of the calorimeter. Therefore, the jet cluster sums are made from the sum of the electromagnetic and hadronic towers in a 2x2 region of trigger-tower space (or 0.4x0.4 in detector $\eta - \phi$ space). Local maxima are required to be separated by one trigger tower and the final energy sums are 4x4 in trigger-tower space.
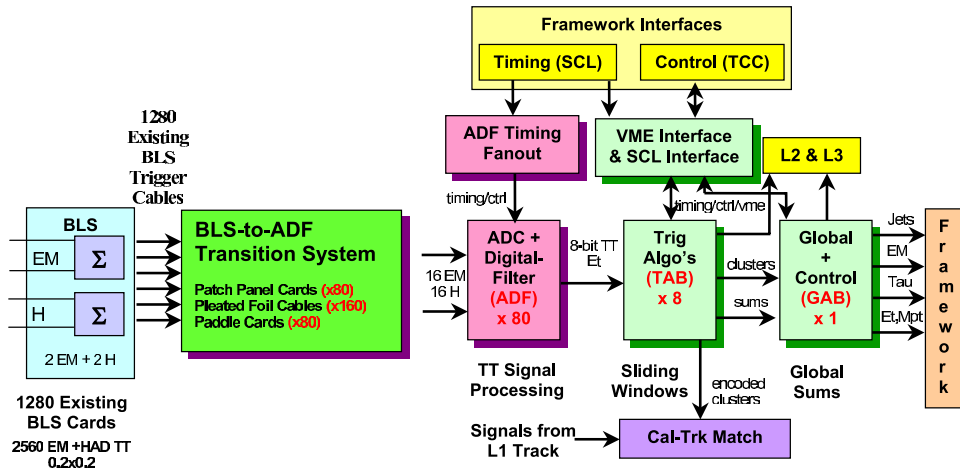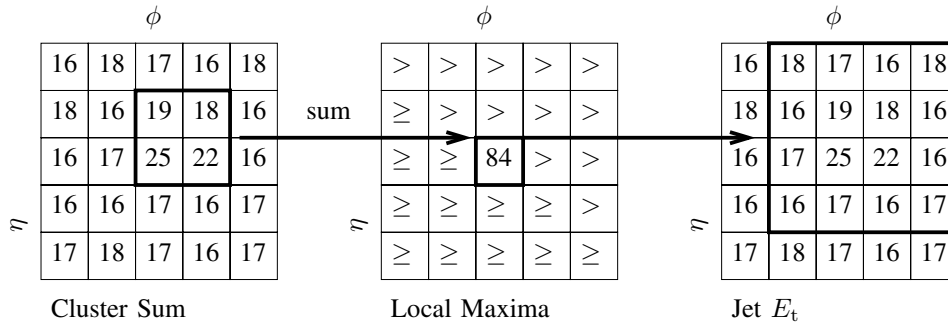
Fig. 1. The Jet Sliding windows Algorithm

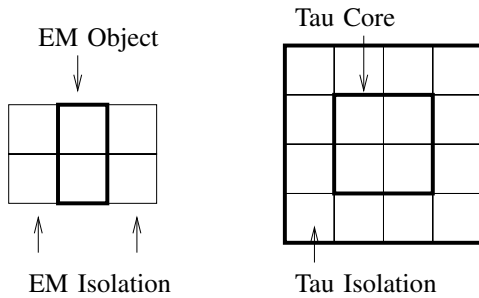Fig. 2. The Jet Sliding Windows Algorithm

Fig. 3. Isolation for EM and Tau Objects

C. Taus

Tau leptons which decay hadronically look similar to jets, but have an energetic core. Therefore, the tau objects are found based on the ratio of the 2x2 cluster sum of a jet object to the 4x4 ring surrounding it (see Figure 3.) The tau objects combine the E_t from the jet algorithm with the ratio of the tau algorithm.

D. Other Triggers

In addition to jets, electrons, and taus, the L1Cal produces scalar and vector E_t sums, counts of single-trigger towers exceeding programmable thresholds, as well as topological terms.

III. ACTIVE ELECTRONICS

The active electronics specially designed for the upgrade includes the ADF, TAB, and GAB cards.

A. ADC plus Digital Filter (ADF) cards (80 single-wide 6U)

The ADF cards receive differential analog trigger energy sums from EM and hadronic calorimeter towers which are digitized energy every 33 ns with 10-bit sampling ADCs. The ADFs output 8-bit filtered, calibrated digital transverse energy sums with least significant bit resolution of 0.25 GeV. The cards are designed for synchronous operation with output every 132 ns.
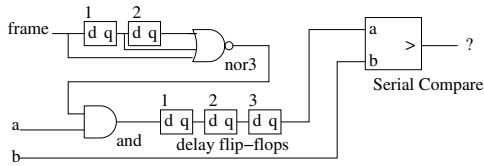
B. Electrons

Electron objects are narrower then jets and tend not to deposit energy in the hadronic calorimeter, so the optimal cluster geometry consists of a single EM trigger-tower (a 1x1 sum). After local maxima finding, the electron object energy is found by adding the trigger-tower energy of the maximal neighboring trigger-tower to create a 2x1 or 1x2 geometry. For isolation, shaping cuts can be applied on the electromagnetic fraction (EM/hadron) and on the ratio of the EM object energy to the energy in the surrounding two 2x1 or 1x2 regions (see Figure 3.)

1393

Fig. 4. A serial divide by 2^3.

Fig. 5. Digital consistency check.

B. Trigger Algorithm Boards (TABs) (8 double-wide 9U)

The eight TABs perform the sliding windows algorithms for the entire 40 η by 32 ϕ grid of trigger tower data. The TAB cards receive digitized transverse energy sums from the ADFs using National Channel Link LVDS at 424 MHz. An FPGA based design calculates the jet sliding windows algorithm with a latency of 230 ns. The cards provide readout at Level 1 using serial-fiber-optic transmission at 1 GHz. This makes the raw trigger-towers available to the Level-2 filter and the event record written to tape. Output to the Caltrk system is accomplished over Muon Serial-Link Daughter Cards at 1 GHz. The TABs are designed for synchronous operation with output every 132 ns, except for the Level-1 readout which is synchronous but at the Level-1 Accept rate.

C. Global Algorithm Board (GAB) (1 double-wide 9U)

The GAB receives regional sums of jet, EM, and tau objects from the TABs over a serial LVDS link at 630 MHz. After being synchronized on four LVDS receiver FPGAs the data from the entire detector is available to one large FPGA which calculates trigger terms. The terms are transmitted to the Level-1 trigger framework using ECL synchronously at 132 ns. Like the TAB, the GAB provides Level-1 readout capability.

IV. SERIAL DESIGN

The sliding windows algorithm requires an irreducibly large grid of input data leading to high-density inputs. This has motivated the widespread use of high-speed serial links for data transport throughout the system.

The sliding windows algorithm is composed primarily of many addition and comparison operations which are easily accommodated by serial logic. With the inputs already serial this leads to a highly compact design. Serial logic makes it possible to use smaller FPGAs at the cost of increasing the clock speed. For a crossing rate of 132 ns, 12-bit serial operation requires a clock speed of 91 MHz, which is easily achievable with modern FPGAs.

A complication arises in the EM and Tau algorithms, both of which require ratio calculations as part of isolation requirements, as described above. The solution for EM isolation requirements is shown in Figure 4. The input serial frame signal (00...01) which marks the least significant bit is sent through delay registers and an XNOR operation to construct a mask (11..1000). Applying an AND of the mask and serial input a, this masks away the three least significant bits: $a_{11}a_{10}\ldots a_3000$. Using 3 delay registers, this is shifted with respect to serial
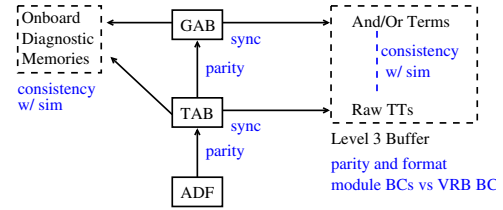
input b to produce $000a_{11}a_{10}\ldots a_3$. When compared to b this now produces the comparison $a/b > 2^3$.

This approach is sufficient for the EM isolation requirements, but the tau algorithm requires greater precision than a 2^n ratio comparison, and a different technique is used.

In this case we want to quickly find $0 \leq a/b \leq 1$ where a and b are 12-bit integers. The inputs a and b deserialized by placing them into shift registers at a cost of 12 ticks. This means that the remaining steps must be very fast to keep the total latency under control. The algorithm counts n leading zeros in denominator b and shifts by this amount to place the 1 in the most significant bit:

$$b = 00\ldots01b_{10-n}\ldots b_0 \qquad (1)$$
$$2^n b = 1b_{10-n}\ldots b_0 00\ldots 0 \qquad (2)$$

With the leading 1 the least significant bits can be neglected at a known loss of precision:

$$1/b = 2^n \cdot 1/1b_{10-n}\ldots b_0 00\ldots 0 \qquad (3)$$
$$1/b \sim 2^{(n-3)} \cdot 1/1x_7 x_6 \ldots x_0 \qquad (4)$$

where $x_7 x_6 \ldots x_0$ are the upper eight bits of $b_{10-n}\ldots b_0 00\ldots 0$. The reciprocal can be quickly retrieved from a lookup table with eight-bit address $x_7 x_6 \ldots x_0$. All that remains is a multiplication by a and a shift for the 2^{n-3} factor to produce output $\sim a/b$.

V. PERFORMANCE

The regimen of consistency checks applied to the digital chain is summarized in Figure 5. For each stage of data transmission, parity and synchronization checks are applied and any errors are latched in status registers. Diagnostic memories are provided to allow comparison of hardware and simulation at each stage of the algorithm calculation. The DAQ readout path contains the raw trigger-tower input and the final trigger terms, allowing for consistency checks of the entire chain for accepted events. During physics running, the status registers are continually monitored and the consistency checks are performed on a subset of the accepted events. During typical operation of the trigger none of these checks detect any errors. One of the more challenging links, the ADF→TAB LVDS transmission, operates with a bit-error rate less than 4×10^{-19}.

The analog performance is best measured by comparing the digitized trigger-pickoff energies to the calorimeter energy measured by the (slower) precision readout path. As shown in Figure 6 there is strong linear correlation for both EM and hadron trigger-towers. We have observed synchronous
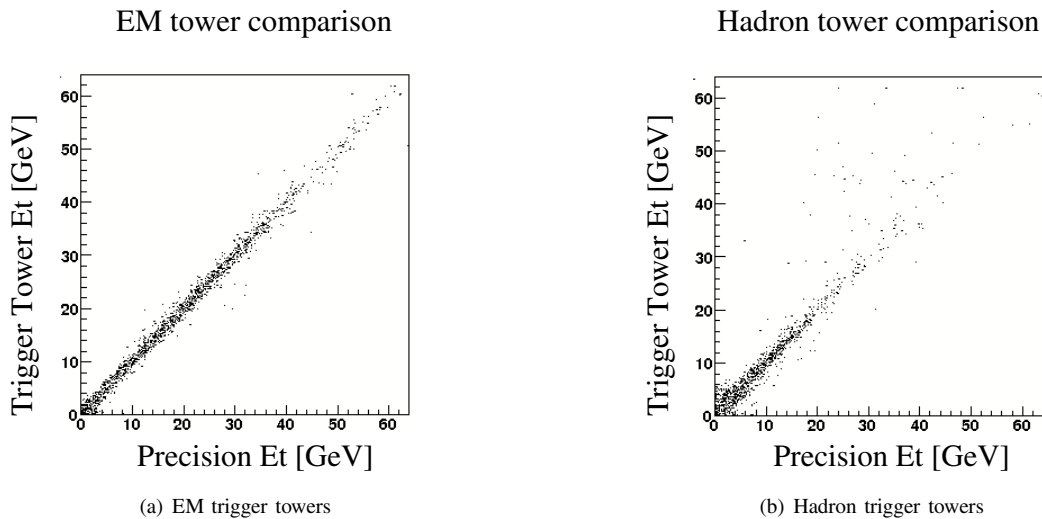
EM tower comparison

(a) EM trigger towers

Hadron tower comparison

(b) Hadron trigger towers

Fig. 6.   Comparison of trigger-towers to precision readout

Run IIA typical jet trigger CJT(1,5)
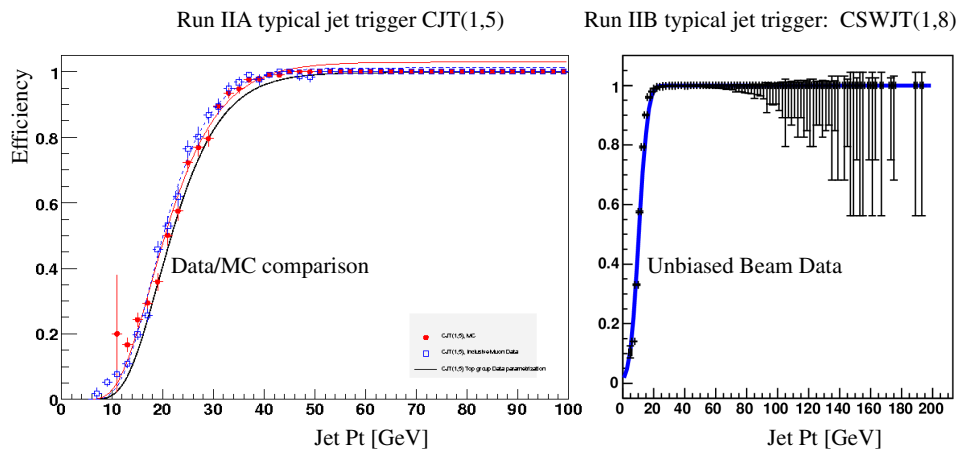
Run IIB typical jet trigger: CSWJT(1,8)

Fig. 7.   Turn-on curves in the upgraded and original trigger

noise on the analog input signals by examining over-sampled data, but fortunately, as the sampling for physics data is also synchronous, this is observed only as a pedestal shift. There are a few exceptional channels that exhibit turn dependent synchronous noise which persists in the physics data, and is currently under investigation.

For physics data taking the most important performance benchmark is the efficiency of the trigger as a function of offline reconstructed object p_t , called turn-on curves. The turn-on curve for a Run IIB term is compared to Run IIA term in Figure 7.

The Level-1 calorimeter trigger was operational within one-half hour of the start of the Tevatron Run IIB. That night, the experts slept soundly, with no pages during the first night of operation. Since the commissioning was completed, the trigger has been running stably, contributing only a few hours to the total DØ dead-time. The new L1Cal has allowed for efficient operation at luminosities that would have broken the Run IIA system.